Access Platforms for Offshore Wind Turbines Using Gratings

Andersen, Thomas Lykke; Rasmussen, Michael R.

Access Platforms for Offshore Wind Turbines Using Gratings

T. Lykke Andersen, M. R. Rasmussen

Department of Civil Engineering, Aalborg University, Denmark

Abstract

The paper deals with forces generated by a stationary jet on different types of gratings and a solid plate. The force reduction factors for the different gratings compared to the solid plate mainly depend on the porosity of the gratings, but the geometry of the grating is also of some importance. The derived reduction factors are expected to be applicable to design of offshore wind turbine access platforms with gratings where slamming also is an important factor.

Keywords: Access platform, offshore wind turbines, gratings, drag forces, mesh screens.

1 Introduction

A large number of offshore wind turbine farms have recently been constructed, more are currently under construction and much more are planned. Therefore, a lot of research is going on within the design of offshore wind turbines and their foundation. If wind turbines are placed in an area with risk of sea ice, an ice cone is typically applied to break the ice by bending which significantly reduce the horizontal force from the ice. The ice cone provides also a platform with access to the wind turbine. In case there is no risk of sea ice a platform consisting of closed plates or gratings has typically been applied. Such platforms using gratings have previously been used for the large wind turbine farm Horns Rev 1 in Denmark, cf. Fig. 1. However, quite some damage has been observed on the platforms and many of the gratings have been dislodged. The damage is expected to be due to larger loads than accounted for in the design. The very large forces are generated by wave run-up along the pile, cf. Fig. 1.

Aalborg University has lately in a wave flume investigated the wave run-up on a circular cylinder and the forces that the run-up generates on a horizontal platform

consisting of solid plates (Lykke Andersen & Brorsen, 2007). These run-up generated forces are typically of very short duration (slamming). The small scale tests were carried out for DONG Energy as a part of the design of the foundations for the planned Horns Rev 2 wind turbine park and for the Horns Rev 1 repair project. The main result of these investigations was a design procedure to calculate the impact pressures on a platform consisting of solid plates.
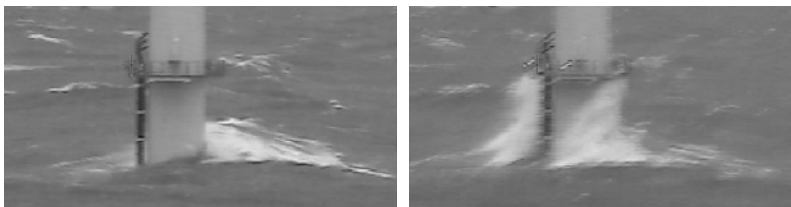

Figure 1. Example of observed run-up event at Horns Rev 1 wind turbine park in Denmark where fiber gratings have previously been used for the platforms.

It is expected that the total force on a platform with grates conservatively can be calculated by applying the reduction factors found for stationary flow to the previously carried out wave flume tests with slamming type impacts. The investigations presented in the present paper deal with estimation of such a reduction factor by measuring forces on a solid plate and four different gratings for an impacting stationary jet. The results presented in the present paper is for flow perpendicular to the gratings only, which is more or less the case for access platforms that are not located at such a low level that they are directly hit by the wave crests.

2 Existing Knowledge

In the present chapter part of the existing knowledge on forces on gratings are presented. As the flow has similarities with the flow around an array of small obstacles, drag forces on small bodies are also considered. The solid plate reference case is discussed as well.

2.1 Drag Forces on Small Bodies

Drag forces on small bodies consist of form drag resulting from pressure differences over the body and skin friction. The relative importance of form drag and skin friction depends strongly on the shape of the body and on the Reynolds number. Skin friction is dominant if there is no flow separation (streamlined body), while form drag is dominant when there are fixed separation points (plate with sharp edges). The drag force is typically calculated using a drag coefficient (C_D):

$$F = \tfrac{1}{2}\rho C_D V^2 A_{ref} \tag{1}$$

The reference area (A_{ref}) is typically taken as the projected frontal area on a plane perpendicular to the flow direction. The drag coefficient is a function of time, Reynolds number, roughness, geometry and turbulence level in the incoming flow.

A body's resistance to flow is strongly affected by its surroundings. A number of experimental results are available with interaction of two and more cylinders. These results generally show an increase in the drag coefficient for two or more cylinders placed side by side when compared to a single cylinder. The enhancement seems mainly to depend on the distance between the cylinders relative to cylinder diameters (the porosity). The flow through a grate has some similarities with that around many small closely placed cylinders.

2.2 Force on Solid Plate

The force exerted on a solid plate hit by a jet can be calculated from the momentum equation:

$$F_x = \rho \cdot Q \cdot \left[V_{x,in} - V_{x,out} \right] \tag{2}$$

where ρ is the density of the fluid, Q is the flow and V_x is the velocity in the x-direction. If we assume that the inflow is perpendicular to the plate and that the outflow is perpendicular to the inflow we get $V_{x,in} = V$ and $V_{x,out} = 0$. From this it can be seen that the solid plate corresponds to $C_D = 2$ as $Q=V \cdot A$ (Morgan, 1962). However, the maximum local pressure is the stagnation pressure corresponding to $C_D = 1$. The reason for $C_D = 2$ on the total force is that the exposed area is larger than the area of the jet.

2.3 Force on Gratings

The above considerations from the momentum equation leads to the force on a highly porous grate must be significantly smaller than that on a solid plate. This is because the main part of the outflow is in the same direction as the inflow. Richards and Robinson, 1999 found for wind loads on porous structures that the reduction for perpendicular attack mainly depends on the porosity (β) defined as:

$$\beta = \frac{V_0}{V_1} = \frac{\text{Area open to flow through grate}}{\text{Total area}} \tag{3}$$

The pressure drop (Δp) across a porous structure depends on the flow resistance through it. The resistance is often characterized by a loss coefficient K, defined in Eq. 4. For structures with high porosity we can assume that most of the flow approaching the porous structure will pass through it and the hydraulic loss coefficient (K) must approximately be equal to the drag coefficient (C_D) (Richards & Robinson, 1999). However, this is only the case if the velocity is taken as the velocity in the incoming jet and the reference area is taken as the total area including the openings (area of jet).

$$K = \frac{\Delta p}{\frac{1}{2}\rho V^2} \qquad (4)$$

In Eq. 4 ρ is the density of the fluid and V is a characteristic velocity. Richards & Robinson, 1999 investigated wind loads on porous structures and gives values of hydraulic loss coefficients (K) for round wire mesh screens as function of porosity and Reynolds number. In addition to the hydraulic loss coefficients Richards & Robinson, 1999 also gives the following function for estimating the relationship between drag coefficients for a solid plate and a round wire mesh screen:

$$C_D = C_{D,Solid} \cdot (1 - \beta_e) \qquad (5)$$

where the reference area used for the drag coefficients is taken as the total area and the velocity used for the porous structure is unclear but here assumed to be the velocity of the jet. The effective porosity β_e takes into account the influence of the geometry and size of the openings. For instance grates made from elements with sharp edges are expected to observe larger forces than elements with rounded edges as observed for single body drag. $\beta_e = \beta$ for round wire mesh screens while $\beta_e = 0.75 \cdot \beta$ for structures made from slats with a depth comparable to their width (Richards & Robinson, 1999). For structures made from flat webs the effective porosity may be about 2/3 of the geometric porosity (Morgan, 1962). This indicates that the rectangular shape has a higher flow resistance than the rounded shapes. In fact, an elliptic shaped bar will only produces 1/3 of the resistance compared to a rectangular bar (Idelchik, 2003). However, in commercial produced grates, this shape is not available.

The wind loading on free standing porous walls with a small size compared to the incoming flow field can be found from (Richards and Robinson, 1999):

$$C_D = 1.2 \cdot (1 - \beta^2) \qquad (6)$$

Annand, 1953 studied the resistance to airflow of wire gauzes. He found that the drag coefficient only is lightly dependant on the Reynolds number for Re > 300 and propose that the drag coefficient can be found as:

$$C_D = \frac{a \cdot (1 - \beta^2)}{\beta^2} \qquad (7)$$

Where a is a Reynolds number dependant coefficient. For high Reynolds numbers, this coefficient becomes constant with a value around 0.55.

For high porosities ($\beta > 0.7$) equations 5, 6 and 7 as well as pressure drop measurements from Idelchik, 2003 gives very similar results, cf. Fig. 4.

3 Model Test Set-Up

The test set-up consists of a frame connected to a large force transducer, cf. Fig. 3. The different grates have been attached to this frame when tested. The force transducer has four sets of strain gauges connected in Wheatstone full bridges by using a strain gauge amplifier. The four voltage outputs from the strain gauge amplifier are linearly dependent on the bending moment in these four points.

The force is measured for a jet generated by a nozzle connected to two large pumps. As the nozzle was placed within few centimeters from the plate/grate the diameter of the impacting jet is very close to the inner diameter of the nozzle equal to 0.081 m. Two pumps of type FLYGT 5.2kW with a maximum flow rate around 35 l/s each have been used for the tests. The flow was measured by a clamp on ultrasonic flow transducer.

Four grates and a solid plate were tested. The dimensions of the different grates are given in Table 1 and pictures are shown in Fig. 2. It can be seen that three of the grates have very similar porosity and only the Weland J9 has a porosity that is significant different from the others. However, the structure of the Fiberline and Weland grates are very different and this might influence the observed forces. The rounded bars used on the Weland grates generally give smaller resistance than bars with sharp edges used for the Fiberline grates.

Table 1. Dimensions of grates and their opening percentage.

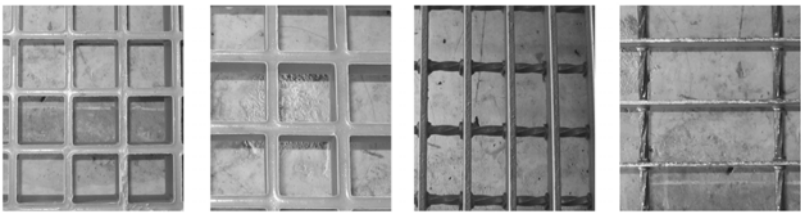| Grate	Openings (mm)	Bar thickness (mm)	Bar depth (mm)	Porosity
Fiberline 40	33.5×33.5	6.5	30	0.70
Fiberline 50	42.5×42.5	7.5	50	0.72
Weland H4 30/5 SAFETY	43.0×28.0	7.0 & 5.5	30	0.72
Weland J9 30/3	92.0×38.0	6.0 & 3.0	30	0.87

Figure 2. Pictures of the four grates used. From left to right is Fiberline 40, Fiberline 50, Weland H4 and Weland J9. The pictures are taken so the grates are viewed from the bottom (the side facing the jet).

4 Results

Pictures of the impact on the four different grates and the solid plate are shown in Fig. 3. It can be seen that the area of the jet is quite small compared not only to the structure of the grates but also compared to prototype conditions. It is possible that this have some influence on the obtained results as the spreading on the rear side of the grate will probably be different if a larger area is exposed. Moreover, the relation between the force on the plate and on the grate might depend on the area considered and the size of the jet. It can be expected that the total force on the platform is well represented by the derived reduction factors while the local forces on the grates might be underestimated by as much as a factor 2. Moreover, the large spreading on the rear side, cf. Fig. 3, indicate no significant downstream suction in the model as it seems well ventilated. As the exposed area is significantly larger in the prototype this might not be true for the prototype conditions.
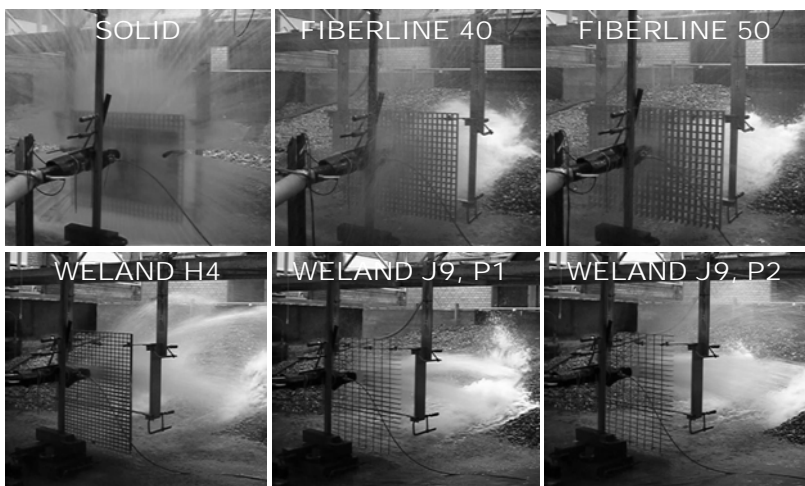

Figure 3. Pictures of impact on the solid plate and the three different grates for close to identical jet velocities.

The large openings in the Weland J9 grate compared to the size of the impacting jet, makes the jet impact point very important. In the present study two positions have been considered, cf. Fig. 3. Position 1 (P1) corresponds to maximum porosity ($\beta \approx 0.95$), while Position 2 (P2) corresponds to minimum porosity ($\beta \approx 0.83$). Moreover, the pictures in Fig. 3 illustrate that for the grates most of the water flow through the grate and has great velocity also behind the grate. This indicates significant smaller forces on the grates compared to the solid plate.

To verify the flow transducer some initial tests were carried out for the solid plate. The results showed C_D values of 1.94 and 2.14 for the two different pairs of electrodes available. This corresponds to only 3% differences in the two flow rates. The results therefore verifies $C_D = 2$ for the solid plate.

In Figure 4 the obtained drag coefficients are compared to the literature values presented in section 2.3. As most of the curves are based on loss coefficients it is important to note that these can only be applied to the present problem for high porosities where the loss and the drag coefficients are close to being identical.

Within the uncertainties related to the experiments, it is clear that the drag coefficient is not strongly dependent on the Reynolds numbers, cf. Fig. 4. However, the tests with the larger flow rate (higher Reynolds number) give generally slightly smaller drag coefficients. This quite weak influence of the Reynolds number simplifies the experiments, as the error conducted by only measuring two jet speeds seems small. This conforms with measurements from Richards & Robinson, 1999.
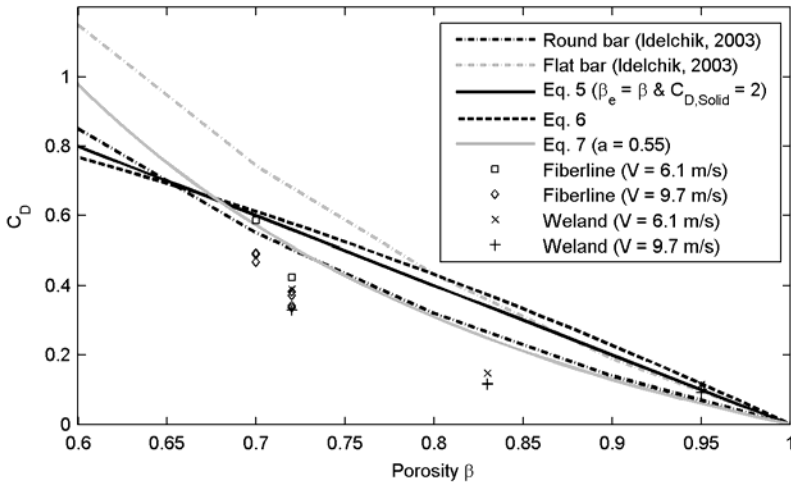

Figure 4. Measured drag coefficients for the different grates.

Comparing the present test results with the literature values for grates, Figure 4, it seems that the measured drag coefficients are in most cases slightly lower than expected. This can maybe be explained by the well ventilated rear side or the very large Reynolds numbers in the present tests. Another explanation could be that even for very porous grates the flow is much different in the present tests compared to the resistance tests. In the present tests this was observed as some part of the water flows parallel with the grate and a small part is even returned in the opposite direction of the impacting jet, which the models based on flow resistance do not consider. Another point is that the downstream suction is probably much different in the two types of experiments. Therefore, the present performed tests are very different to a grate submerged in a stationary flow where all of the water has to flow through the grate. This also explains why the curves based pressure loss coefficients starts to diverge strongly at porosities lower than 0.7.

The jet in the prototype is expected to be much larger than tested in the experiments but smaller than the extension of platform. Therefore, it seems relevant later to investigate the influence of the size of the grate compared to the size of the jet, especially when the force on a single grate is considered.

Fig. 4 shows that the drag coefficient is mainly dependent on the porosity of the grate but also the geometry of the grate elements is of importance. Comparing the four different grates studied here, suggests that the two Fiberline grates give drag coefficients that are higher than those for the Weland grates. This is expected mainly to be due to the rounded bars used for the Weland grates instead of the sharp edged slats used for the Fiberline grates. Grates with sharp edged elements correspond to a smaller effective porosity, cf. section 2.3.

It is clear from the results in Fig. 4 that Eq. 7 seems to be a quite safe design line in most cases. However, the uncertainties related to the small jet in the experiments compared to the prototype have to be taken into account. Moreover, slamming has to be considered separately.

5 Conclusions

The jet generated forces on four different grates and a solid plate have been measured. The results show that the use of grates instead of solid plates for access platforms will reduce the forces significantly. The reduction seems mainly to depend on the porosity of the grates but also the geometry of the grate is important. The forces measured for the two tested Fiberline grates (porosity approx. 70%) is approximately 25% of that on a solid plate. The Weland grates generally observe smaller forces than the Fiberline grate even for close to identical porosity. This is expected to be due to the use of rounded elements instead of sharp edged elements.

A number of important issues have not been considered in the present investigations, but might be very important, i.e. the direction of the jet, the size of the exposed area and the reduction factors for slamming forces compared to the stationary flow case. However, the determined reduction factors are expected to be conservative with respect to the total slamming force on the platform.

References

Annand, W. J. D. (1953). The Resistance to Air Flow of Wire Gauzes. *Journal of the Royal Aeronautical Society,* Vol. 57, p. 141-146.

Idelchik, I. E. (2003). Handbook of Hydraulic Resistance. *CRC Begell House*.

Lykke Andersen, T. & Brorsen, M. (2007). Horns Rev II, 2-D Model Tests. Impact Pressures on Horizontal and Cone Platforms from Irregular Waves. *DCE Contract Report No. 13, Dept. of Civil Eng., Aalborg University.*

Morgan, P. G. (1962). Flow through screens of low solidity. *Journal of the Royal Aeronautical Society*, Vol. 66, p. 54-56.

Richards, P. J. & Robinson, M. (1999). Wind Loads on Porous Structures. *Journal of Wind Engineering and Industrial Aerodynamics* 83, p. 455-465.